Do the homework and explore galaxy collisions

G. Arreaga-García

Departamento de Investigación en Física, Universidad de Sonora, Apartado Postal 14740, 83000, Hermosillo, Sonora, Mexico.

Received 25 September 2024; accepted 17 December 2024

In this paper we test a code to model the collision of galaxies. This code is based on the program GALAXY, which is proposed in Appendix J of a well-known textbook in astrophysics. The GALAXY program is in turn based on the approximation model proposed by the Toomre brothers in 1972. With this model, it was possible to demonstrate very efficiently that the tails and bridges observed by astronomers when two galaxies collide have their origin in the gravitational tidal forces. We have made several improvements to our code with respect to the one described in Appendix J, such as (i) the possibility of evolving more than two galaxies (up to N-galaxies); (ii) the placement of stars in each of the galaxies; (iii) the rotation of the galaxies according to Euler angles; and finally, (iv) coding in ansi c rather than the original Basic language. To test the code we ran the binary collision models proposed in the homework part of the book, namely the whirlpool and cartwheel models. Then we rotated the galaxies involved in the collision and examined the differences in the results. To generate more models we change the initial velocity of the disturbing galaxy. We found geometrically and physically more interesting star configurations. In addition, we ran the Stephan model with five interacting galaxies. To show the final results of the models, we use our own algorithm to perform a density smoothing procedure and create two-dimensional isodensity plots with `Python`. To give the reader the opportunity to practice and visualize the different scenarios, the source programs are shared in the link: `https://drive.google.com/drive/folders/1J08YVJICYWbAZbSGceO-uOZtNrCmC7Op?usp=sharing`.

Keywords: Galaxies: kinematics and dynamics; galaxies: interaction; methods: numerical.

DOI: https://doi.org/10.31349/RevMexFisE.23.010204

1. Introduction

The results of the NASA/ESA Hubble Space Telescope are so spectacular that they have attracted the attention of the public. In 2024 alone, many reports have appeared in national newspapers relating to collisions between galaxies, see [1]. The first new item is about the collision between the galaxies NGC 6040 and LEDA 59642, see Fig. 1. It was mentioned that "galactic collisions and mergers are monumentally energetic and dramatic events, but occur on a very slow timescale". It was also mentioned that the structures of the galaxies change a lot during the collision "due to the enormous changes in the gravitational forces acting on them". Both comments are true and indeed, in this paper we show in more detail some of the physics behind such interesting phenomena, through an exhibition suitable for the general public.

A high percentage of the observed galaxies are elegant, and have beautiful disk and spiral shapes. But other galaxies are not like this and are referred to as peculiar galaxies. The origin of peculiar galaxies, as shown and described in the newspaper's reports [1], with deformed bodies and long tails, has long been a mystery.

A starting point for young students in this field of science is provided by the textbook [2], which provides a general introduction to the area and includes a GALAXY code in Appendix J. The GALAXY code is based on the idea of the Toomre brothers, see [3]. In this groundbreaking work, they presented an approximate model for a galaxy. Such a model consisted of many stars in orbit around a central point mass. They considered two galaxies interacting gravitationally, so that the central masses exert an attractive force on each other and on all the stars. The stars did not interact gravitationally with other stars. Using this model they were able to produce the tails and bridges that were observed by astronomers, and whose origin was debated at the time. The Toomre paper made a major contribution to clarifying this area. This is a brilliant example of using a physical approach to discover the nature of more complicated phenomena. They helped solve the mystery of the origin of peculiar galaxies: these are the result of one or more collisions between galaxies.

In this paper, we have recreated the GALAXY code in a modern programming language. At that time, the authors

FIGURE 1. Image taken from the newspaper "La Jornada" of January 13, 2024.

used the Basic language to manage the plots as a result of the code. Nowadays, we use ansi c and the results can be better created in `Python`, to take advantage of the graphical capabilities. Using this code, we completed the exercises sugggested at the end of Chapter 24 of [2] and we present that results in this paper.

We have added some improvements to the GALAXY code. The first is that our code can handle more than two galaxies, whereas the code proposed in Ref. [2] only considered two galaxies. The second is that we place stars around all the central points involved, while in Ref. [2] the stars are only placed around one galaxy. The third is that we can rotate the system of galaxies using the Euler angles formalism.

We clarify that this method for studying galaxy collisions is already part of the heritage of physics. Although research is still being carried out today in the modeling of galaxies and galaxy collisions, more complete techniques are used, and therefore there are more difficult to implement for a student, see for example [4].

The structure of the paper is as follows. In Sec. 2, we show the type of galactic systems to be simulated with this approximate code. In Sec. 3, we show the stellar configuration obtained by running the code with initial conditions motivated by the real systems described in Sec. 2. In Sec. 4 and 5, we discuss the relevance of our results and make some concluding remarks.

2. The physical systems and computational considerations

In this section, we briefly describe some well-known physical systems that have been extensively modeled using various computational methods. We decided to test our code with these systems in order to validate it by comparing it with other papers. We mention the geometric setup of the collisions of each model. In the next section, we will show the results of the modeling.

2.1. The whirlpool model

The first system is known as the Whirlpool galaxy, see Fig. 2. The setup to simulate this system consists of a main galaxy of mass 10×10^{10} $M_\odot$ and a disturbing galaxy of mass 2.5×10^{10} $M_\odot$ that are separated by 90 kpc. The two galaxies are in the same plane, which is chosen as the XY plane. The main galaxy is at rest at the origin of a Cartesian coordinate system while the disturbing galaxy is approaching (or moving away from) the main galaxy with a velocity of 136 km/s. This setup and its two variants, to be defined below, represent an oblique galaxy collision.

2.2. The cartwheel model

A second exercise proposed in the Section of Problems of Chapter 24 of [2] has to do with the so-called Cartwheel galaxy, see Fig. 3. The setup for this system consists of two equally massive galaxies of mass 10×10^{10} $M_\odot$, which are separated by 70 kpc along the Z axis. The galaxy located in the XY plane is at rest, and we call it the target. The galaxy located in a higher plane (but still parallel to the XY plane) is directed towards the target galaxy with a velocity of 400 km/s. We call this the projectile galaxy. This setup represents a head-on galaxy collision.

We will also consider a variant of the cartwheel model, as follows: [7] has studied this galaxy and considered the case in which the projectile galaxy is much smaller than the target galaxy. This makes sense, because the Cartwheel galaxy is part of a small group of galaxies, it is then possible that the projectile galaxy was one of those companion galaxies, which are smaller than the Cartwheel.

FIGURE 2. The Whirlpool galaxy. Image taken from the Wikimedia Commons.

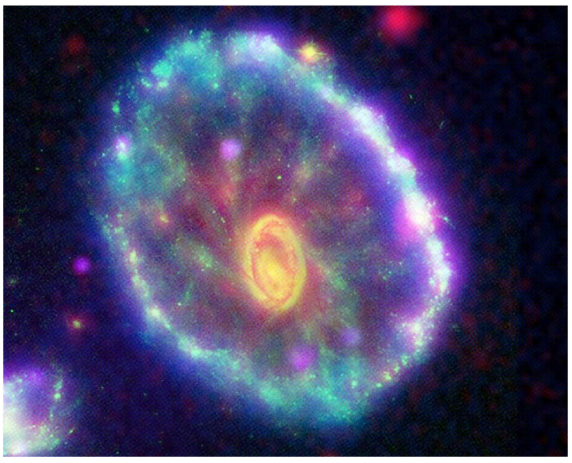

FIGURE 3. The Cartwheel galaxy. Image taken from the Wikimedia Commons.

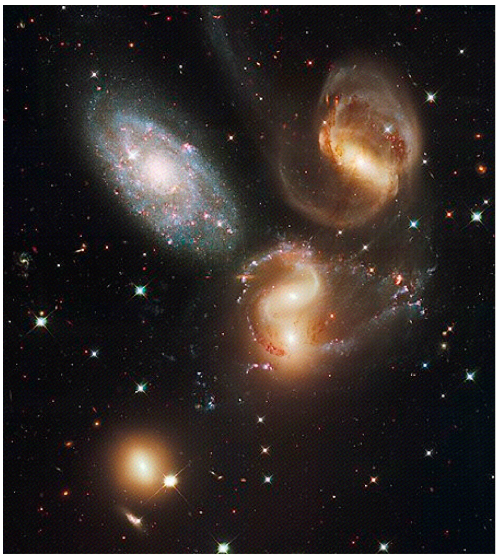

FIGURE 4. The Stephan quintet model. Image taken from the Wikimedia Commons.

2.3. The Stephan model

A third exercise to test the code, which is not suggested in the book, consists of a small group of 5 galaxies, called Stephan's quintet, see Fig. 4. This group was studied by Hickson and he included it in his catalog of compact groups with the label group 92, see [5]. The galaxies have a mass factor different, as follows: 6, 3, 1.5, 1.0 and 0.5. The mass of each galaxy can be obtained by multiplying this factor by a base mass of 2×10^{10} $M_{\odot}$. The galaxies are distributed in an almost linear curve as suggested by numerical simulations, see [16]. The initial distances between the galaxies of the group are shown in Table I.

The masses, positions, velocities and angles were taken from observations, but some values are still subject to uncertainty, see [8].

2.4. The code

As we have already mentioned, we are testing here our own code, which is based on the one shown in Ref. [2]. The main idea behind these codes is an approximate model of a galaxy as a dimensionless point of mass, surrounded by a series of concentric rings. The rings are circles lying in a plane that represent the spatial extent of the model galaxy. This arrangement represents a spiral galaxy. The number of rings is a parameter of the code. We use 50 rings for the models to be considered in Sec. 3.

TABLE I. The distances between galaxies in the Stephan model.

galaxy	galaxy	distance [kpc]
1	2	73.93
1	3	116.54
1	4	42.44
1	5	14.16
2	3	42.73
2	4	31.73
2	5	87.90
3	4	74.36
3	5	130.57
4	5	56.35

A second parameter of the code is the number of stars per ring. Let us explain the meaning of a star for the code. Each ring can have a certain number of dimensionless point particles. It must be emphasized that the stars have no gravitational influence on the system. However, the motion of the stars is influenced by the gravitational pull of the central point of mass. This is possible because the acceleration of each star is affected by the gravitational force of the point masses. The mass of the stars would appear on both sides of the Newton's second law of motion and therefore the mass of the stars would cancel out in the equation of motion.

For this reason, it is to be expected that the number of stars per ring has no influence on the results of the system evolution. This number is only used for better visualization. In the case of the models of Sec. 3, we use 500 stars per ring. It must be mentioned that the book suggests using fewer rings and fewer tars per galaxy. Furthermore, in the book's code, only one galaxy has stars, while the other galaxy has none. We believe that these suggestions were implemented to make the code of that time more efficient. Nowadays, such restrictions are no longer necessary.

This computational system will evolve in time over a certain number of time steps. This is another parameter of the code: the total number of time steps. During the time evolution, the separation between particles can become very small or even zero. Therefore, the gravitational force would have an arbitrarily large magnitude, and cause an overflow problem in the computer. To avoid this, a softening length with a value of 2 in code units (which corresponds to 1 kpc in physical units) has been included in both codes.

Finally, there are two parameters of the code that control the geometry of the galaxy, namely the radial extent of all rings and the radius of the first ring (the innermost ring of the galaxy). For the whirlpool model, we use the values 20 and 10 as suggested in the book (which corresponds to a size of 10 kpc and 5 kpc). For the Cartwheel model, we reduce the second parameter from 10 to 5. For the Stephan model, we use 50 rings with 250 stars per ring, so we have 12500 stars in the model.

3. Results

3.1. The whirlpool model

In Fig. 5 we show two snapshots of the resulting configuration of the whirlpool model. Initially, the disturbing galaxy is located at the coordinates (30, -30, 0) in units of the code,

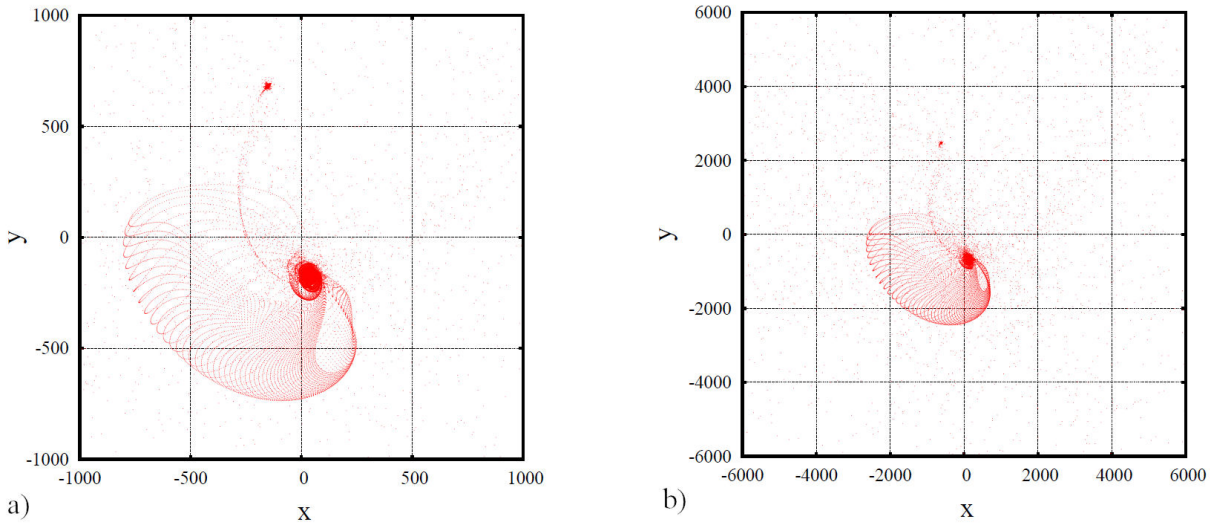

FIGURE 5. Time evolution of the whirlpool model. The time (in millions of years) for every panel is as follows: a) 6, b) 21.6.

i.e., in the fourth quadrant of the coordinate system (with coordinates $x > 0$ and $y < 0$) and the velocity is (0,0.34,0.34) in units of the code. Rapidly, the disturbing galaxy moves up to the second quadrant (with coordinates $x < 0$ and $y > 0$) during a brief period of 1.2 million years. It must be noted that the disturbing galaxy circled through the entire first quadrant (with coordinates $x > 0$ and $y > 0$). In the meantime, the main galaxy has moved a little away in the negative direction along the Y-axis. The left panel of Fig. 5 shows the configuration of the system after 6 million years. The disturbing galaxy is still in the second quadrant and one can see the bridge of stars connecting the two galaxies. In addition, one can see that the star system has expanded spatially forming a closed surface. The right panel shows the configuration of the system after 21.6 million years. This configuration is basically the same configuration as in the left panel, but many stars have moved very far away with respect to the galaxies. For this reason, the scale of the coordinate axes has greatly increased, a sea of stars fills the space. In this plot, a point represents a star, see [9]. The comparison of this resulting configuration with Fig. 2 is immediate.

3.2. Variants of the whirlpool model

We now consider variants of the whirlpool model to illustrate that the resulting configurations can be very different. For example, we move the initial position of the disturbing galaxy to (150,100,0) in units of the code, and the initial velocity is still (0, 0.34,0.34) in units of the code. It must be noted that the velocity vector of the disturbing galaxy points outwards and therefore it tries to move away from the main galaxy. In Fig. 6 we show the results of our code for the new whirlpool setup. In the top left panel one can see the main galaxy with practically no changes to its initial configuration. The disturbing galaxy located in the right corner of the panel, already shows an extension of its initial star configuration after 2.4 millions of years. In the next panels of this Fig. 6 one can see that the stars of the disturbing galaxy are under a strong attractive force caused by the main galaxy, so that many stars of the disturbing galaxy move towards the main galaxy through two matter channels. In the lower-right panel of Fig. 6, one can see that one of these matter channels finally touches the main galaxy after 9.6 millions of years.

A clarifying note is in order. The plots shown in Fig. 6 were created with a software that allows the system to be freely rotated to view the 3D structure, see [10]. In this type of plots, the axes have been rotated so that a different view can be selected from panel to panel in the same figure.

We now consider a rotation of the initial galaxy system, by using the formalism of Euler angles, described by [11]. In this formalism, three angles are defined: ϕ, indicating a rotation around the Z axis; θ for a rotation around the new X-axis and finally, ψ for a rotation around the new Z-axis. It should be noted that only two angles are required for a meaningful rotation of the galaxies, see for example the definition of the angles i and w of [3]. For the main galaxy we consider the angles (given in degrees) ϕ, θ ψ = 0, 30,30 while those of the disturbing galaxy are ϕ, θ ψ = 0, -30,-30, see the right panel of Fig. 7 and compare with the left panel of Fig. 7.

As can be seen in Fig. 8, the resulting dynamic of the rotated system is more interesting, as the arms of stars are more elongated and twisted than those observed in Fig. 9. In addition, the main galaxy has shown more activity than in the case without rotation. In the left-top panel of Fig. 8, one can see that the stars of the main galaxy start to move to form an "S structure", which is clearly visible in the upper-right panel. The arms of stars from the disturbing galaxy reach the main galaxy at two points, as seen in the lower left and right panels of Fig. 8.

In Fig. 6 and 8 we focus on the star configurations and therefore the physical scale of the system is not clear. It must be noted the significant separation of the galaxy centres after 9.6 millions of years. In the length units of the code, the ini-

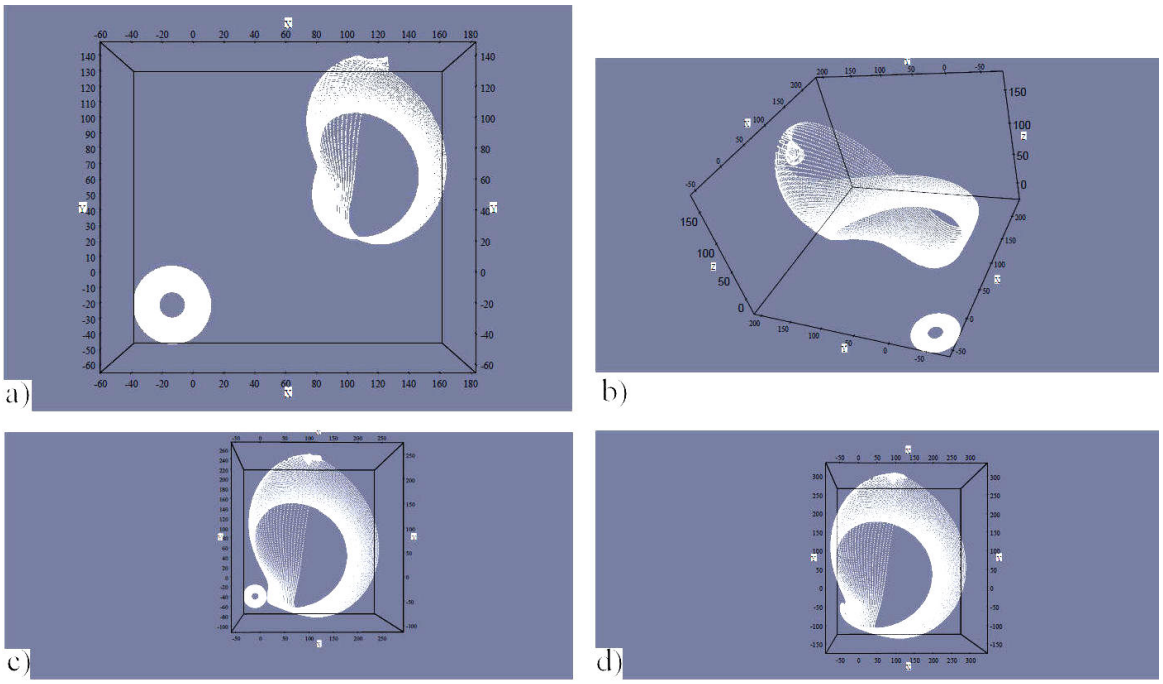

FIGURE 6. Time evolution of the first variant of the whirlpool model. The time (in millions of years) for every panel is as follows: a) 2.4; b) 4.8; c) 7.2, and d) 9.6.

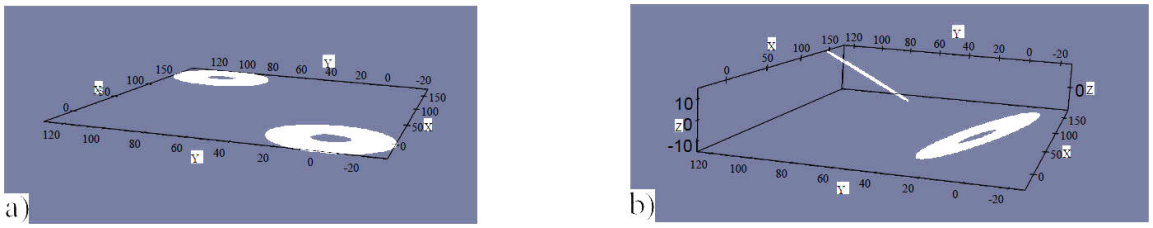

FIGURE 7. a) The initial galaxies of the first variant of the whirlpool model b) have been rotated.

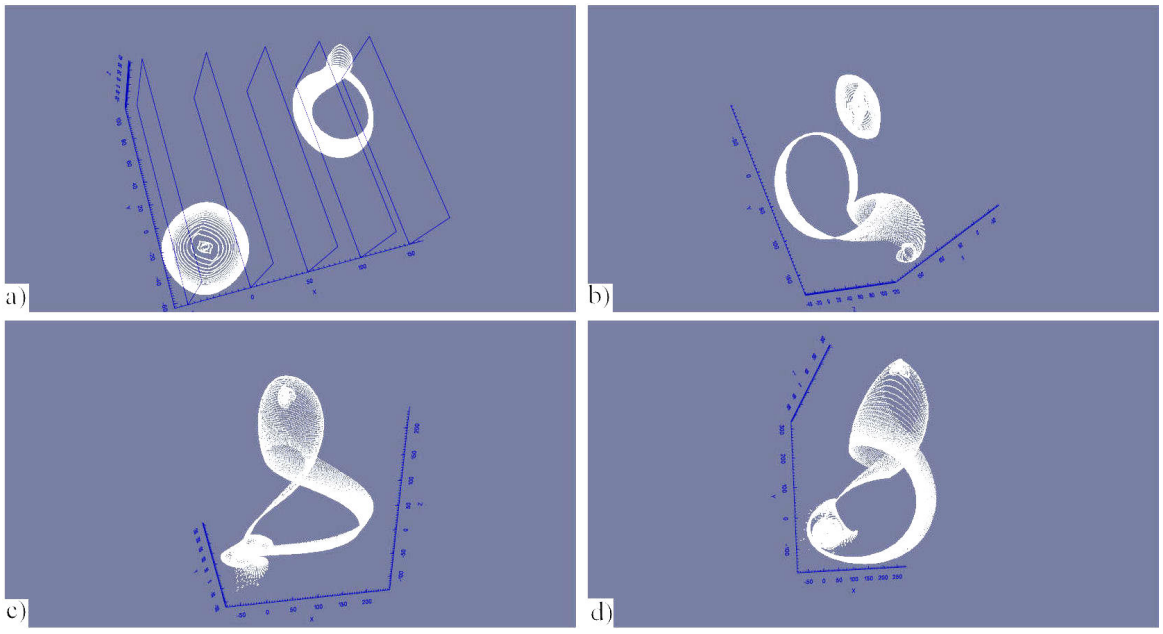

FIGURE 8. Time evolution of the rotated first variant of the whirlpool model, whose initial galaxies have been rotated with respect to that of the model illustrated in Fig. 6. The time (in millions of years) for every panel is as follows: a) 1.2; b) 3.6; c) 7.2 and d) 9.6.

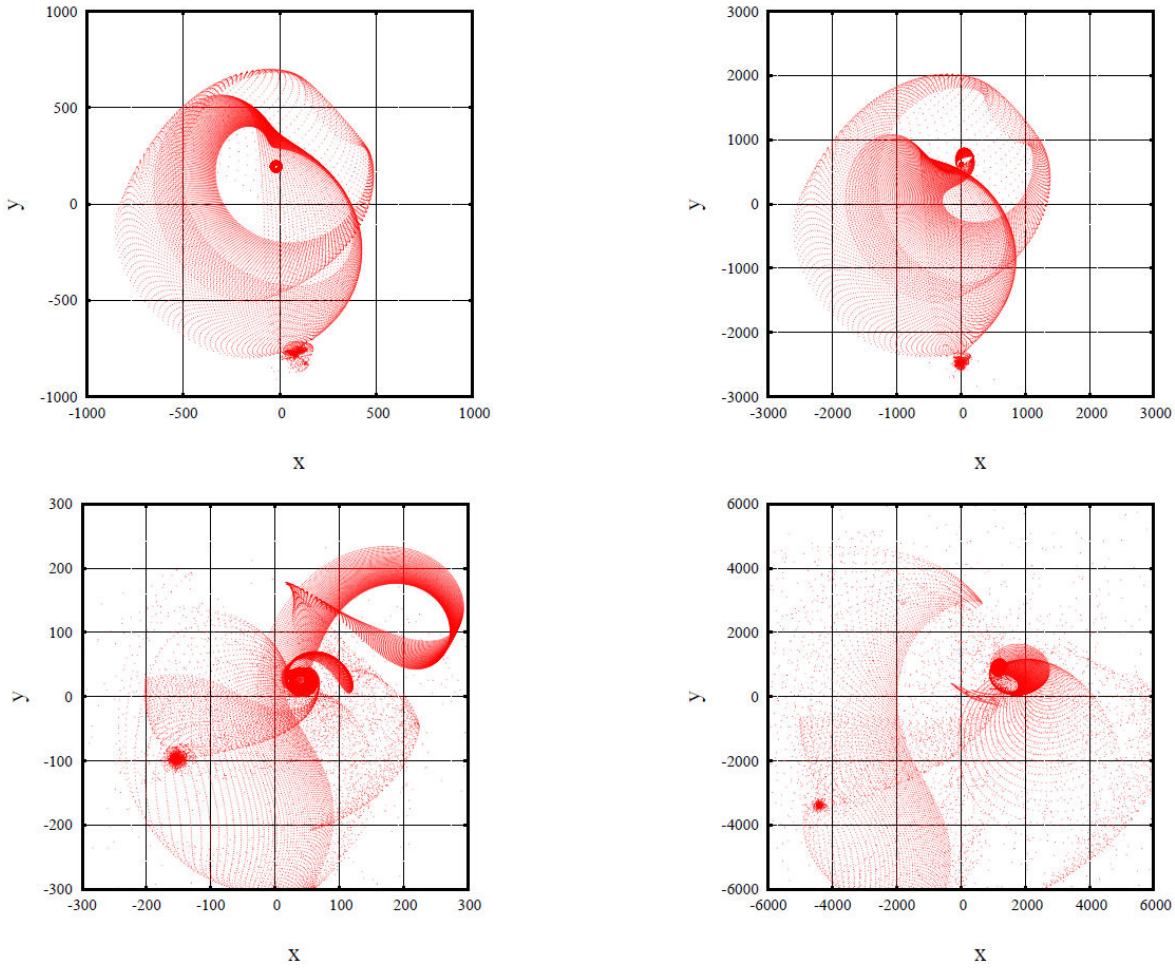

FIGURE 9. Time evolution of the second and third variants of the whirlpool model. The time (in millions of years) for every panel is as follows: second variant, a) 7.2; b) 21.6; third variant: c) 1.2 and d) 21.6.

tial separation was illustrated in a plot with a width of (-150 to 150) on the x-axis and a width of (-20 to 120) on the y-axis. After 9.6 millions of years a width of (-200,400) in both axes is needed to cover the stellar configuration. Therefore, the system has expanded to double the space it initially occupied.

Let us now consider a change in the direction of the initial velocity vector of the disturbing galaxy. The second variant of the whirlpool model consists of the same initial configuration of the galaxies, *i.e.*, (150,100,0) but the velocity vector of the disturbing galaxy points in the opposite direction of the first variant of the whirlpool model, *i.e.*, the components of the velocity are now (0,-0.34,-0.34), in code units. The third variant consists of the same initial configuration as the first and second variants of the whirlpool model, with the exception of the velocity vector of the disturbing galaxy, which has doubled in magnitude towards the negative values of the X-axis, *i.e.*, the components of the velocity are (-0.68,-0.34,0) in code units. A schematic representation of the variant models is shown in Fig. 10 to summarize the different variants of the whirlpool model.

To save space, we will present the results of both variations in the same Fig. 9, as follows. The two panels of the top row for the second variation and the panels of the bottom row

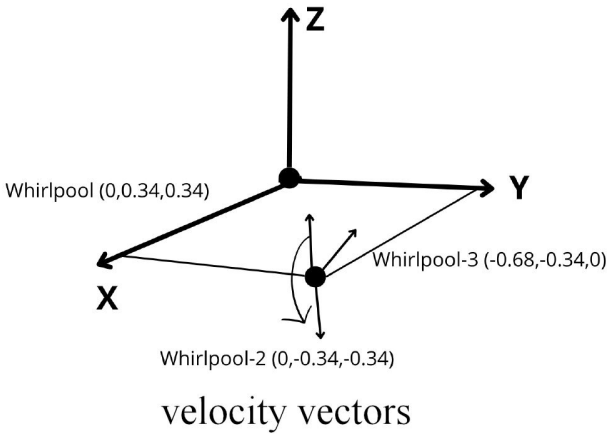

FIGURE 10. Schematic representation of the variants of the whirlpool model. The only change is in the velocity vector of the disturbing galaxy. The components of the velocity are shown next to the name in Cartesian coordinates.

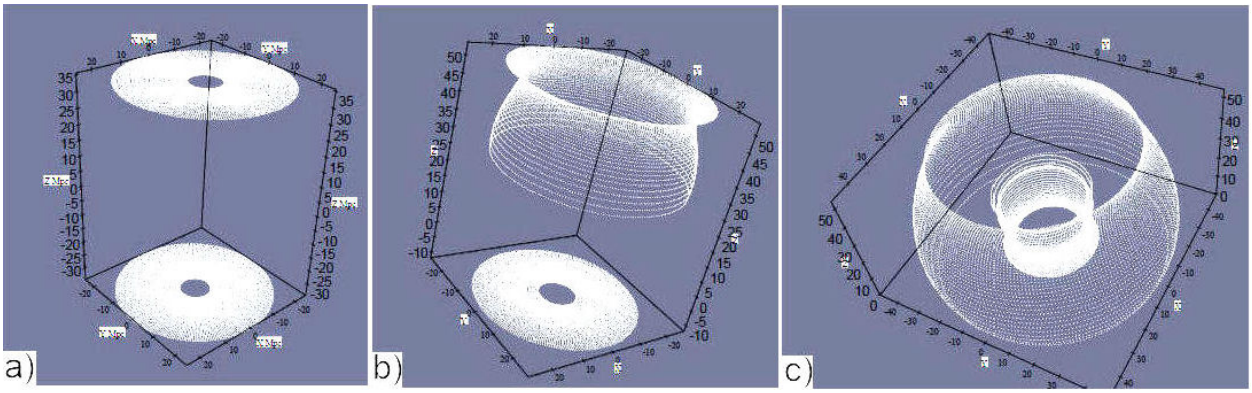

FIGURE 11. Time evolution of the cartwheel model. The time (in millions of years) for every panel is as follows: a) 0; b) 4.8; c) 9.6.

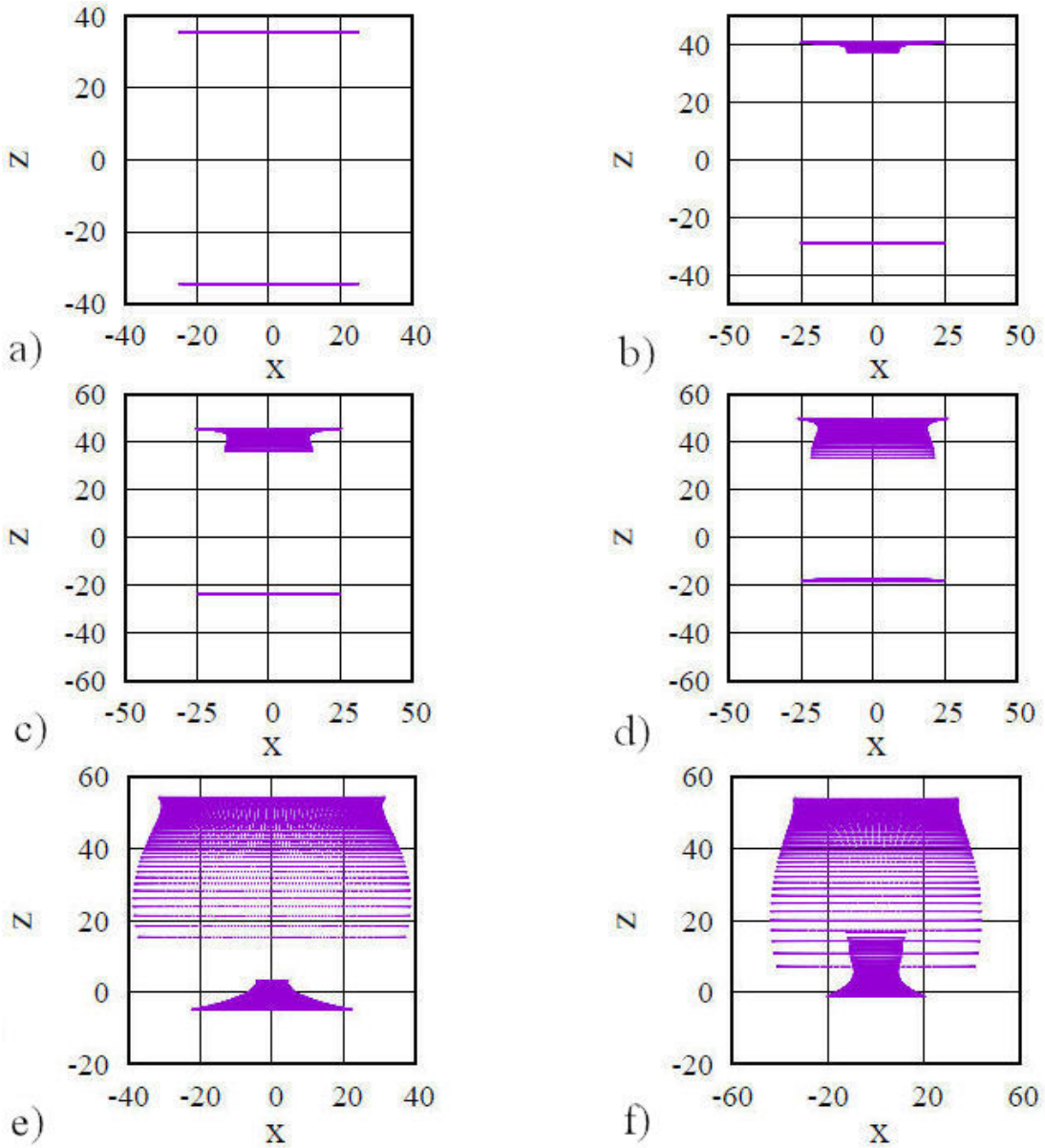

FIGURE 12. Time evolution of the cartwheel model, by looking at planes parallel to the ZX plane. The time (in millions of years) for every panel is as follows: a) 0; b) 1.2; c) 2.4 and d) 3.6; e) 7.2 and f) 8.4.

for the third variation. In the two panels of the left column of Fig. 9 we see that the two galaxies in the variants are moving reasonably well, as they have followed the trajectories expected of a two-body problem. For the second variant, the disturbing galaxy is below and to the right (in the fourth quadrant with coordinates $x > 0$ and $y < 0$) of the main galaxy while in the third variant the disturbing galaxy has rounded the main galaxy from above (in the third quadrant with coordinates $x < 0$ and $y < 0$). The two panels of the right column show the last snapshot of each variant taken at 21.6 million of years. In the case of the second variant, the display of the stars is impressive. They seem to stretch without limit. In the case of the third variant the development of bridges and tails is notable.

3.3. The cartwheel model

We have run another model that represents a head-on collision between two equal-mass galaxies. In Fig. 11 we show the time evolution of this model. The initial configuration can be seen in the upper panel. It consists of the galaxies located one above the other, so that the projectile galaxy moves downwards and charges on the target galaxy located below. For the separation suggested in the book, the collision occurs very quickly. For this reason, we have used twice the initial separation between the galaxies, 70 kpc.

After 4.8 millions of years, in the middle panel of Fig. 11 one can see that stars of the projectile galaxy form concentric rings whose radius increases towards the bottom. At the same time, the stars of the target galaxy show no disturbance. In the bottom panel of Fig. 11, after 9.6 millions of years, the view of the system is from the positive Z-axis, one can see a concentric series of rings coming from both galaxies. In Fig. 12 we show the alternative plots that completed the time evolution shown in Fig. 11. One can note the change in physical scale of the system.

We now consider a rotation of the initial galaxy system of the cartwheel model. We use only one Euler angle, $\theta = 45$. This rotation was only applied to the projectile galaxy, as one can see in the upper-left panel of Fig. 13. In the upper-right panel of Fig. 13 one can see that the projectile galaxy is ejecting stars due to the gravitational force caused by the target galaxy. These stars do not retain the concentric rings as was the case in the system without rotation.

As usual, we supplement the illustration of the results with the dot plots, shown in Fig. 14. In the upper-left panel of Fig. 14 one can see that the target galaxy remains unchanged, while the stars of the projectile galaxy begin to move downwards. The stars of the projectile galaxy take on a configuration reminiscent of a cocoon in which the target galaxy is embedded, see the last two panels of Fig. 14.

3.4. Variant of the cartwheel model

Following [7], we now consider that the projectile galaxy is smaller in size and mass than the target galaxy. The initial radius of the target galaxy is 30 and for the projectile galaxy the radius is 10. The mass of the projectile galaxy has been chosen to be 0.2 the mass of the target galaxy, as was done by Citeata. In Fig. 15 we show the results of this model.

3.5. The Stephan model

In the upper-left panel of Fig. 16 we show the initial distribution of galaxies at time 0. There are 5 galaxies and they are

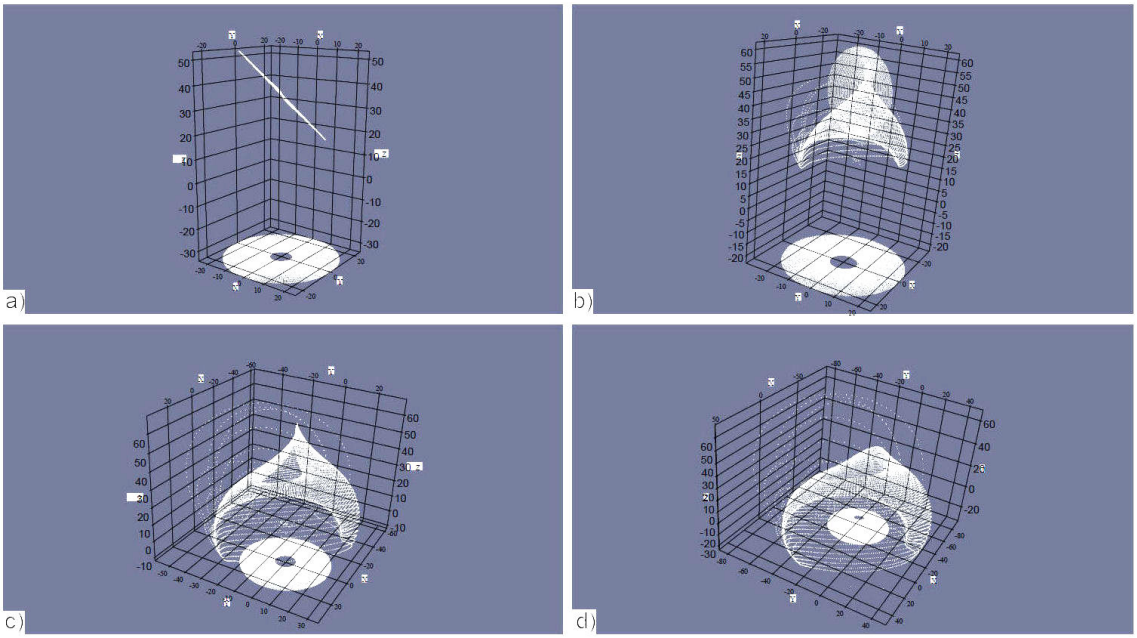

FIGURE 13. Time evolution of the rotated cartwheel model. The time (in millions of years) for every panel is as follows: a) 0; b) 2.4; c) 4.8 and d) 7.2.

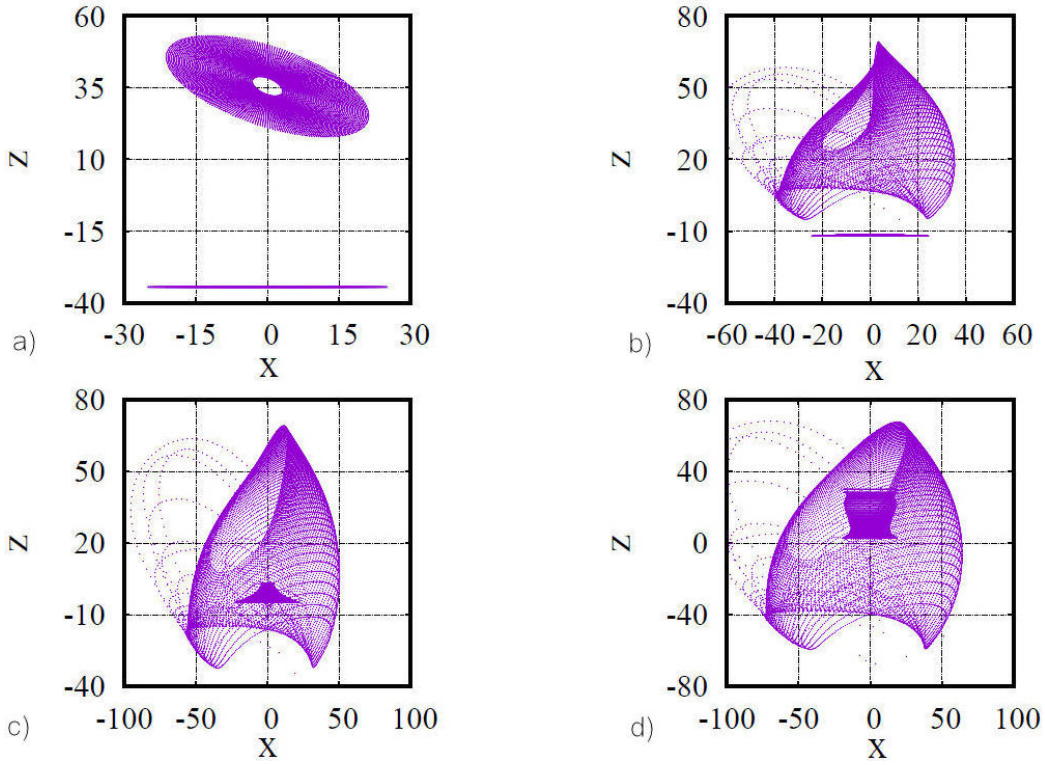

FIGURE 14. Time evolution of the rotated cartwheel model, by means of planes parallel to the ZX plane. The time (in millions of years) for every panel is as follows: a) 0; b) 4.8; c) 7.2 and d) 9.6.

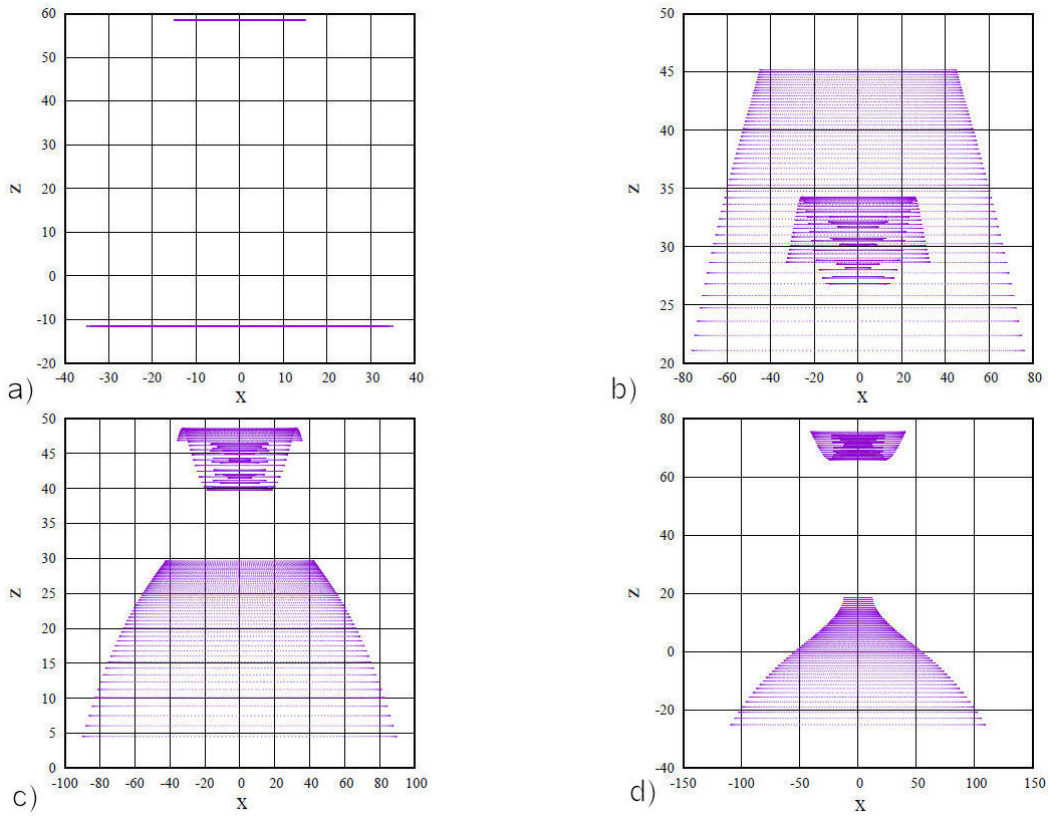

FIGURE 15. Time evolution of a variant of the cartwheel model, by means of planes parallel to the ZX plane. The time (in millions of years) for every panel is as follows: a) 0 (the initial conditions); b) 10.8; c) 14.4 and d) 21.6.

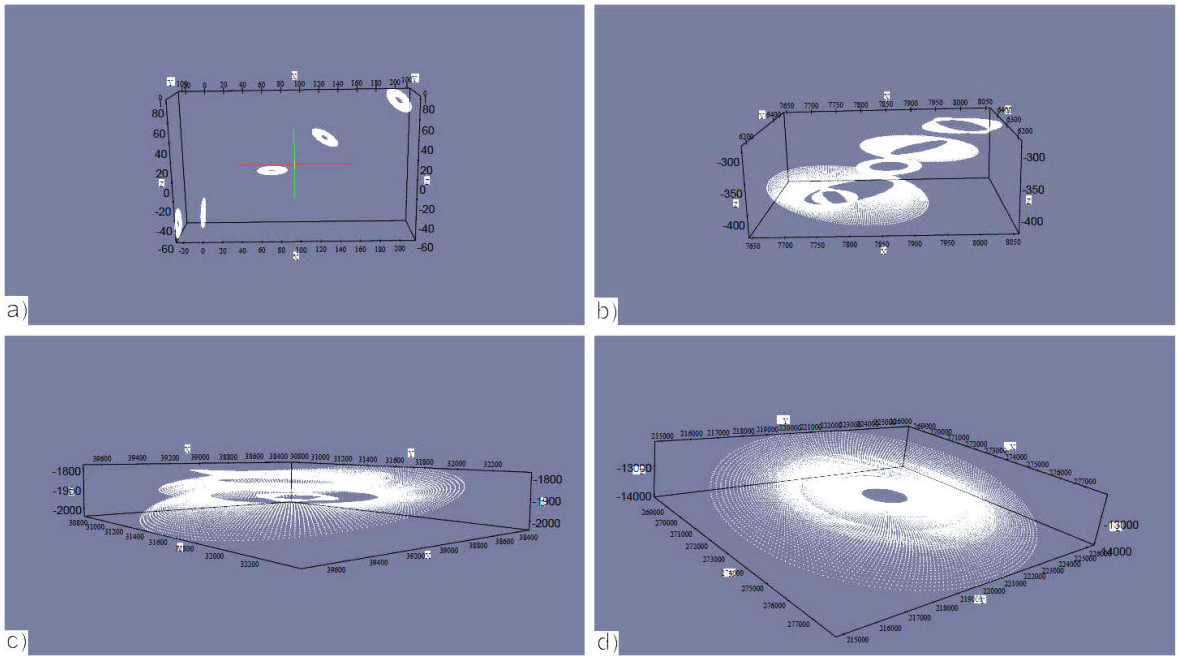

FIGURE 16. Time evolution of the Stephan model. The time (in millions of years) for every panel is as follows: a) 0; b) 1.2; c) 6 and d) 42.

grouped in a subgroup with three members and a second subgroup with two members. It should be noted that each member has been rotated. In the upper-right panel of Fig. 16, we see that the stellar disks begin to distort and expand rapidly. This plot corresponds to a time of 1.2 million years. In the lower-left panel of Fig. 16 we see that the galaxies begin to stack over a period of 6 million years. This stacking process continues, and we have followed it up to a time of 42 million years, as can be seen in the right-bottom panel of Fig. 16.

3.6. The final results of the models

To show the final result of a simulated model in a representation that makes sense to an astronomer, a smoothing procedure must be applied to a snapshot. As we have already mentioned, in the previous figures, a dot represents a star. As we have seen, the stars are distributed in three spatial dimensions. Astronomers can normally only see plane or spherical projections in two spatial dimensions. We then briefly describe the smoothing process.

For the whirlpool model, consider the plots at the bottom-right panel of Fig. 6 and 8, which represent the last snapshots obtained without and with rotation, respectively. They show the spatial configuration of the stars after 9.6 million years of the model evolution. We applied the smoothing procedure to these files.

We read the position of the stars in the Cartesian coordinates (x, y, z) and ignore the third coordinate z. We then place a two-dimensional grid over the resulting star projection (x, y). This grid has 64 cell elements in each coordinate axis X an Y. The total number of cell elements in the grid is therefore 4096.

We count the number of stars in each cell element n_i and calculate the distance of each star to the centre of the cell d_i. Then we normalize the distance with half the width of the cell, σ_0. We approximate the density of each grid element $< \rho >$ using the following Gaussian smoothing function $< \rho >= \Sigma_i \left(m_i \exp(d_i/\sigma_0)\right)$. In this equation, i ranges from 1 to 4096, m_i the mass of the star and Σ_i indicates that the sum is over all the particles of the cell.

Since it was not necessary to specify the mass of the stars m_i, we can now use the arbitrary value 1 and speak of the density per unit mass, or alternatively, think of the density in arbitrary units. In any case, it is most important to compare the values on the color scale, shown in the vertical bar on the right side of the plots.

Thus, for each cell element of the grid, we store the smoothed density. These numbers are used for a `Python` code to create a plot, in which it is given the coordinates of the centre and the smoothed density. The resulting plots are shown in Figs. 17, 18 and 19.

Analogously to the whirlpool model, we now show the final plots of the cartwheel model, after the application of the same smoothing procedure to the snapshots shown in the bottom panel of Fig. 11 for the case without rotation and to the right-bottom panel of Fig. 14 for the case of rotation. These plots represent the star configuration after 9.6 million years of the evolution of the model. The resulting plots are shown in Fig. 18. Finally, we show the density plots for two evolution times of the Stephan model, see Fig. 19. These panels correspond to the ones shown in the bottom line of Fig. 16.

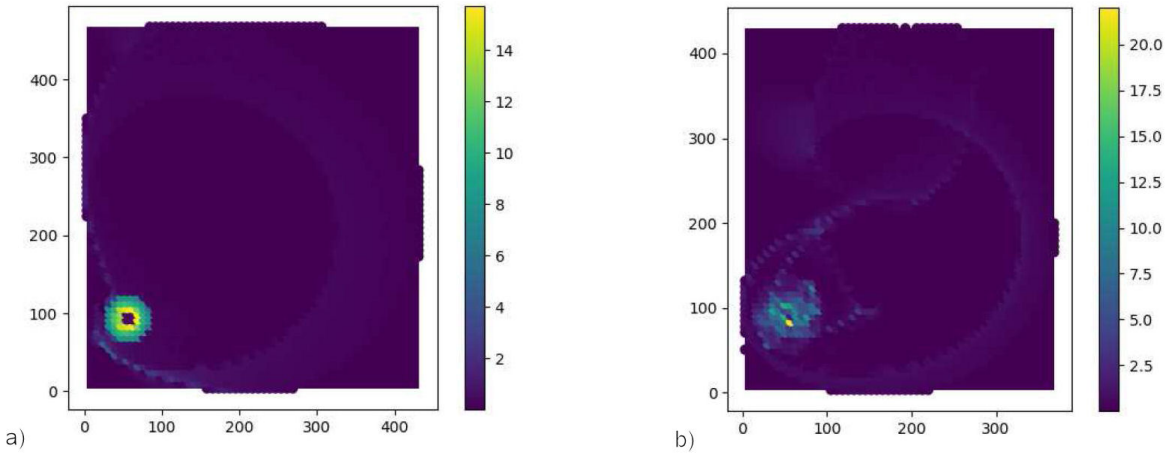

FIGURE 17. The resulting smoothed density for the whirlpool model. a) Represents the model without rotation and b) represents the model with rotation.

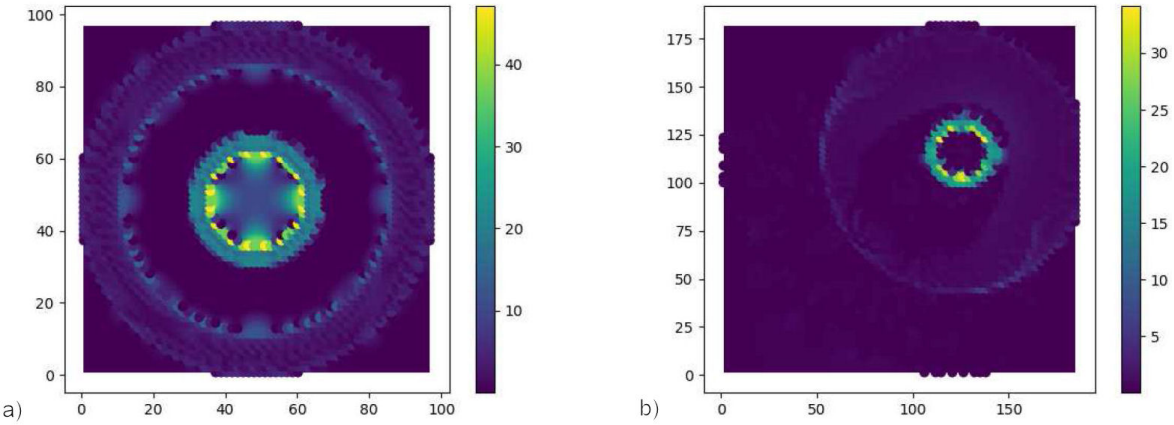

FIGURE 18. The resulting smoothed density of the Cartwheel model. a) Represents the model without rotation and b) represents the model with rotation.

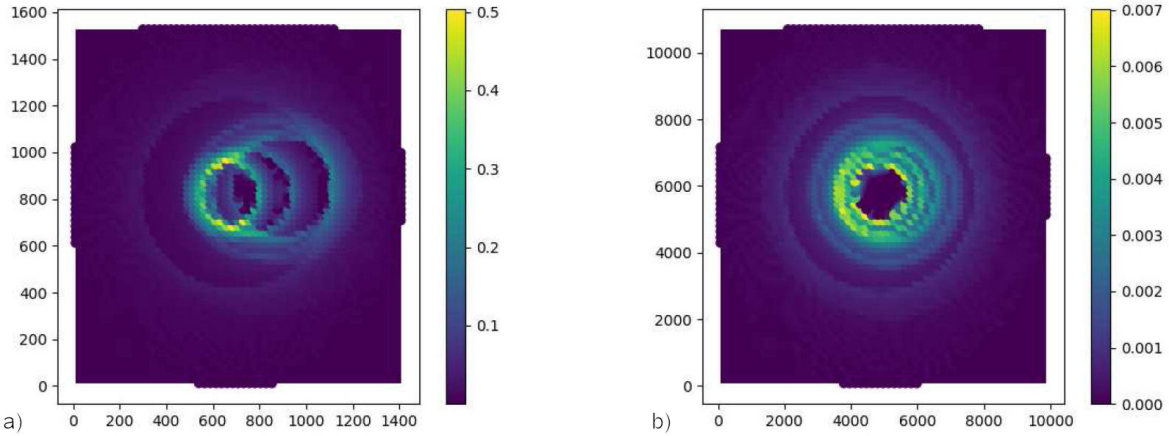

FIGURE 19. The resulting smoothed density of the Sthephan model. a) Represents the model at 6 millions of years and b) represents the model at 42 millions of years.

4. Discussion

The initial conditions of the classical galaxy models, *i.e.*, the whirlpool and the cartwheel models, were proposed by the authors of the original code in the book of [2]. For these models, we show interesting stellar configurations from a geometrical point of view. The comparison with the physical models shown in Sec. 1 is immediate. Therefore, the results

shown in Sec. 3 allows us to validate the performance of the code as we obtained the expected configurations. Then, this code can become a tool to experience new collision models, as we have done in the models shown in Sec. 3.

It must be noted that we have given the models plenty of time to evolve, but for limitations of space, we have illustrated some models very sparsely. The characterization of the stellar distribution in physical and geometric terms is not discussed here for reasons of space and is reserved for a future publication. Below, we will emphasize some points of the models.

4.1. The whirlpool model

We have considered several variations of the classic whirlpool model in order to illustrate the enormous differences in the resulting star configurations. At the initial time, the differences between these variants and the classic whirlpool model were: (i) the disturbing galaxy is located initially further away; (ii) the initial velocity vector of the disturbing galaxy has changed.

These variant models are characterized by the formation of wide branches of stars connecting the main and the disturbing galaxies. In the case of the first variant of the whirlpool model with and without rotation, accretion is the main process. Accretion is clearly evident as two long arms of stars form from the disturbing galaxy towards the main galaxy. The results in the rotated models are visually more interesting. It must be noted that the main galaxy shows different behavior with respect to whether the disturbing galaxy is rotated or not. In the non-rotated case, the gravitational force between the galaxies is almost vertical, since the component in the plane of the main galaxy is very small. But in the rotated case, the gravitational force has a larger component in the plane of the main galaxy.

In the first variant of the whirlpool model, the main galaxy was barely affected. In the second and third variants of the whirlpool model there is a noticeable movement of the main galaxy. In addition, long bridges of stars have appeared.

4.2. The cartwheel model

In the case of the cartwheel model with and without rotation, the expansion of the stellar configuration is clearly visible. This motion is a consequence of the conservation of momentum of the system, as follows. The initial momentum of the system is clearly directed along the negative values of the Z axis, since the projectile galaxy has a translation velocity in that direction while the target galaxy has no momentum. Initially, the total momentum in the plane parallel to the XY plane must be zero. When the stars of the projectile galaxy approach the target galaxy, the stars in the projectile galaxy must move radially outward in pairs, in order to keep the system having zero momentum in the plane parallel to the XY plane. As expected, the results in the rotated models are visually more interesting.

4.3. The Stephan model

In the case of the Stephan quintet, we only saw the stacking of galaxies. The initial conditions do not seem to be very relevant, since the final product of the evolution will be a stacked system of galaxies. It is interesting to note that the disk structure of the galaxies is preserved. In more complete simulations, which include dark matter halo and bulge, it is seen that the collision of spiral galaxies leads to galactic systems with elliptical distribution. In this calculation, we have followed the evolution of this model up to just over 42 million years. Perhaps we need to follow the evolution up to hundreds of millions of years to see the formation of an elliptical galaxy as a result of the collision of this 5-galaxy system.

5. Concluding remarks

In this paper we have tested a new code to simulate galaxy collisions. The code is based on the approximate model of [3]. Although this model is very old, simulations based on this model allow students to quickly gain physical intuition. Galactic dynamics is a field of research with a very old history, and yet there are still open problems that need to be considered, see [12].

The main product of this paper is a tested and validated code based on that code kindle provided in the Appendix J of the book [2]. The code passes dynamic tests so it looks reasonable. Since this code can be run on a laptop, it is an easy way to motivate students to explore the field of galaxy collisions. Students can investigate different physical configurations, and calculate the conservation of linear momentum, angular momentum and other physical properties. Furthermore, a geometric characterization of the stellar structure can be an interesting task. For instance, [13] presents a catalogue of observed ring-shaped galaxies, and other rather rare galaxy configurations. It would be interesting for students to select some of these ring galaxies and run numerical models to understand their main physical properties.

Another proprietary tool we developed for this work was the code for smoothing the star distribution in terms of approximate density. We tried to summarize the result of a numerical model by means of this smoothing process and make the comparison with observations more plausible.

The dynamics of galaxies during collision has become a very important digital tool for science education and teaching, see for example [14]. On this website, users were invited to participate in the classification of galaxies and the generation of galaxy collisions so that the results could be seen immediately. More recently, a virtual observatory with a database of galaxy collisions has been presented in Ref. [15].

Of course, this is an approximate method. To go beyond this approximation, a lot of hard work is required. A self-consistent galaxy model must be created, that includes several components, such as a bulge of stars, the disk formed by stars, the dark matter halo and gas, see for example [6] and

references therein. Such a model must be evolved on a supercomputer and using a parallel code as the GADGET, see [17]. The reward for this effort is that we can simulate star formation, see for instance [18–20]: and galaxy formation, see for instance [16].

Acknowledgements

The author gratefully acknowledges the computer resources, technical expertise and support provided by the Laboratorio Nacional de Supercómputo del Sureste de México through grant number O-2016/047.

1. La Jornada: Noticia del 13 de enero del 2024: Hubble capta colision monstruosa de galaxias. Noticia del 24 de mayo del 2024: Hubble captura la galaxia espiral NGC 4689 y Noticia del 13 de julio del 2024: galaxias entrelazadas.
2. B.W. Carroll and D.A. Ostile, *An introduction to Modern Astrophysics*, 2nd ed., (Addison-Wesley, 1996).
3. A. Toomre and J. Toomre, Galactic bridges and tails, *Astrophys. J.*, **178** (1972) 623-666.
4. R. Bottema, Simulations of normal spirals galaxies, *Mon. Not. R. Astron. Soc.*, **344** (2003) 358-384. https://doi.org/10.1046/j.1365-8711.2003.06613.x
5. P. Hickson and C.M. Oliveira, J.P. Huchra and G.G.C. Palumbo, Dynamical properties of compact groups of galaxies, *Astrophys. J.*, **399** (1992) 353-367.
6. G. Arreaga-García, A thick-disk galaxy model and simulations of equal-mass galaxy pair collisions, *Res. Astron. Astrophys*, **20** (2020) 189, https://dx.doi.org/10.1088/1674-4527/20/11/189
7. A. Bosma, Models of the Cartwheel Galaxy, In M. Valtonen and C. Flynn, eds., *Small Galaxy Groups ASP Conference Series*, **174** (2000) 255, https://doi.org/10.1017/S0252921100055081
8. Wikipedia, 2024, https://es.wikipedia.org/wiki/Quinteto_de_Stephan.
9. http://www.gnuplot.info/documentation.html
10. Paraview https://www.paraview.org/
11. H. Goldstain, *Classical Mechanics*, 2nd ed. (Addison-Wesley, 1980).
12. R. C. Kennicutt, Jr., F. Schweizer and J. E. Barnes, *Galaxies: Interactions and induced star formation*, (Springel, 1996). https://doi.org/10.1007/3-540-31630-2
13. B. Madore, E. Nelson and K. Petrillo, *Atlas and catalogs of collisional ring galaxies*, *ApJS*, **181** (2009) 572-604.
14. https://www.zooniverse.org/projects/zookeeper/galaxy-zoo/ and https://blog.galaxyzoo.org/.
15. I.V. Chilingarian, P. Di Matteo, F. Combes, and A.L. Melchior, and B. Semelin, Astronomy and Astrophysics, **518** (2010) A61, https://doi.org/10.1051/0004-6361/200912938
16. G. Arreaga-García, Empirical formulae to describe some physical properties of small groups of protogalaxies with multiplicity, *Res. Astron. Astrophys*, **21** (2021) 198, https://dx.doi.org/10.1088/1674-4527/21/8/198
17. V. Springel, The cosmological simulation code GADGET-2, *Mon. Not. R. Astron. Soc.*, **364** (2005) 1105, https://doi.org/10.1111/j.1365-2966.2005.09655.x
18. G. Arreaga-García, J. Klapp, L.D. Sigalotti and R. Gabbasov, *Gravitational collapse and fragmentation of molecular core cloud with GADGET-2*, *ApJ*, **666** (2007) 290, https://dx.doi.org/10.1086/520492.
19. G. Arreaga-García, *The formation mass of a binary system via fragmentation of a rotating parent cloud with increasing total mass*, *Rev. Mex. Astron. Astro.* **52** (2016) 155,
20. G. Arreaga-García, *Comparing binary systems from rotating parent gas structures with different total masses*, *Astrophys. Space Sci.*, **362** (2017) 47, https://doi.org/10.1007/s10509-017-3028-9